Paper No.
04736

CORROSION2004

CO_2 CORROSION IN THE PRESENCE OF TRACE AMOUNTS OF H_2S

Bruce Brown, Shilpha Reddy Parakala, Srdjan Nesic
Institute for Corrosion and Multiphase Technology
Ohio University
Athens, Ohio 45701

ABSTRACT

Experiments were conducted to determine the effect of an incremental change in the solution pH, from 4 to 6.6, on CO_2 corrosion rates of AISI 1018 steel in the presence of H_2S in both single phase flow (V_{sl} = 1 m/s) and multiphase flow (V_{sg}=3 m/s, V_{sl}= 1 m/s) in a large scale multiphase flow loop. Linear polarization probes, electrical resistance probes, and weight loss coupons were used to monitor corrosion rates during 4 to 10 day exposures to a CO_2 saturated solution with trace amounts of H_2S. The media for experimentation was a 1% NaCl solution at 60ºC, at 7.9 bar (100 psig) total pressure, with gas phase additions of H_2S up to 100 ppm. Protective adherent films, seen under these conditions, limited corrosion rates in both single phase and multiphase flow conditions.

Keywords: hydrogen sulfide, carbon dioxide, acid gas, multiphase flow, single-phase flow, saturation

INTRODUCTION

In order to develop a better understanding and prediction tools for CO_2/H_2S corrosion in the future, it is imperative that the basic corrosion mechanisms are well understood. A dedicated study is considered necessary where the basic electrochemical mechanisms of CO_2/H_2S corrosion of bare mild steel will be revisited. This will produce a healthy platform for studying the effect of other complicating parameters, such as formation of protective surface scales, effect of inhibitors, hydrocarbons, glycols, methanol, and condensation in wet gas transport and multiphase flow.

Some early research[1] in this field has suggested that a low concentration of H_2S (<30 ppm) in a CO_2 saturated water solution can accelerate the corrosion rate significantly in comparison to corrosion in

Copyright
©2004 by NACE International. Requests for permission to publish this manuscript in any form, in part or in whole must be in writing to NACE International, Publications Division, 1440 South Creek Drive, Houston, Texas 77084-4906. The material presented and the views expressed in this paper are solely those of the author(s) and not necessarily endorsed by the Association. Printed in U.S.A.

a similar CO_2 environment without H_2S. This "H_2S effect" seemed to vanish at higher H_2S concentrations and higher temperatures[1,2] (>80°C) when a protective film forms. In a Norwegian study[3] it was suggested that this effect of H_2S could be significant only in the low pH range (<pH 5).

In general, the reasons behind the "H_2S effect" on CO_2 corrosion are not entirely understood. It has been speculated that adsorbed sulfide species and/or sulfide films affect the corrosion rate of mild steel through a catalytic or a galvanic effect[3]. All of the previously conducted studies have largely ignored the effect of flow (with the exception of Kvarekval[3] who conducted experiments at room temperature and low pressure).

From our own research,[4] there seems to be enough evidence about the effect of very small H_2S concentrations on CO_2 corrosion at low pH, where precipitation of iron sulfides does not occur. For concentrations of H_2S below 500 ppm in the gas phase and for pH<5, a large number of carefully controlled corrosion experiments have been conducted over the past few years, at various temperatures (20-80°C), partial pressures of CO_2 (1-7 bar) and velocities (stagnant to 3 m/s) in both single and multiphase flow. All the data strongly suggest that the presence of even very small amounts of H_2S (10 ppm in the gas phase) will lead to rapid and significant reduction in the CO_2 corrosion rate. At higher H_2S concentrations this trend is somewhat reversed (see Figure 1). The effect seems to be universal and depends solely on the H_2S concentration, as all the data obtained at very different conditions follow the same trend. The corrosion rate in Figure 1 was normalized with the "blank" corrosion rate, i.e. a CO_2 corrosion rate obtained without any H_2S present.

In the present study, experimental parameters were chosen to cover a range of parameters leading to iron carbonate ($FeCO_3$) and iron sulfide (FeS_{1-x}, mackinawite) precipitation. The concentration of H_2S and the solution pH, at a constant temperature and constant partial pressure of CO_2, were altered to adjust the bulk solution saturation of both mackinawite and iron carbonate from "under-saturated" at pH 4 to "super-saturated" at pH 6. The solubility product for mackinawite ($K_{sp(FeS)}$) was calculated using

$$pK_{sp(FeS)} = 2848.779/T - 6.347 \qquad (1)$$

with temperature(T) in Kelvin, by Benning, et al.[5]. The bulk saturation value for mackinawite, denoted as $S(FeS_{(1-X)})$, was calculated from the equation:

$$S_{FeS_{(1-X)}} = \frac{\left[Fe^{+2}\right]\left[HS^{-}\right]}{\left[H^{+}\right]K_{sp[FeS_{(1-X)}]}} \qquad (2)$$

The solubility product for iron carbonate, ($K_{sp(FeCO_3)}$), was calculated using the equation:

$$pK_{sp(FeCO_3)} = 10.13 + 0.0182(T) \quad (3)$$

with temperature(T) in ºC. The equation for solubility constant of iron carbonate was taken from IUPAC[6] because the effect of ionic strength on the solubility constant could be neglected for 1% NaCl solution. The bulk saturation value for iron carbonate, S($FeCO_3$), was calculated from the equation:

$$S_{FeCo_3} = \frac{\left[Fe^{+2}\right]\left[CO_3^{-2}\right]}{K_{sp[FeCO_3]}} \quad (4)$$

The equations were used to calculate the saturation values for varying concentrations of iron in solution. These theoretical curves for iron carbonate saturation and iron sulfide saturation at pH 4, 5, and 6 are shown in Figure 2. Notice that mackinawite (FeS_{1-X}) would be supersaturated at pH 5 for iron concentrations greater than 20 ppm.

Hence, the following experiments were conducted to better understand the corrosion mechanisms at high temperatures and high pressures in H_2S environments under bulk supersaturation conditions for both $FeS_{(1-X)}$ and $FeCO_3$. In addition, this kind of basic data is indispensable for development of more reliable mechanistic CO_2/H_2S corrosion models.

EXPERIMENTAL PROCEDURE

The procedure for operating the large scale multiphase flow loop or Hydrogen Sulfide System was described in a previous study[7]. All experimental parameters, such as pH, temperature, partial pressures, and iron concentration, were adjusted and/or measured for stable conditions prior to the insertion of all flush mounted probes. The experimental parameters chosen for the study of corrosion in the presence of trace amounts of H_2S are shown in Table 1. Parameter variations during the operation of this flow loop were expected and adjustments were made as required. Concentration of H_2S varied up to 20% of the desired concentration during testing due to consumption and re-introduction. Solution pH was maintained within ± 0.2 pH units of the required value by addition of an acid (HCl) or a base ($NaHCO_3$) during operation. As shown in Figure 3, the iron concentration was observed to increase with time in the case of pH 4 due to corrosion, and to decrease with time for experiments at pH 5, 6, and 6.6 due to precipitation.

The current series of tests were conducted in a 1% NaCl solution at 60ºC. A three-electrode probe in a concentric ring arrangement was used for linear polarization resistance (LPR), a retrievable large flush mounted element for high pressure access systems was used for electrical resistance (ER), and an arrangement of four 0.457" diameter mild steel coupons for weight loss (WL) were used to monitor corrosion rates during the 96-hour (4 day) exposures to this CO_2 saturated solution with trace amounts of H_2S. LPR and AC impedance measurements were taken using an electrochemical measurement system and the concentric ring probe. The H_2S system was used to provide a very stable

environment for reproducible flow rates in single phase and multiphase flows. The single-phase flow is at a liquid velocity of 1.0 m/s while the multiphase flow is at 3.0 m/s superficial gas velocity and 1.0 m/s superficial liquid velocity to produce slug flow. Corrosion rates from each method will be compared, along with surface analysis of the WL coupons, to provide a better understanding of the H_2S effect over the area of interest. The WL material's chemical composition is given in Table 2.

The experimental parameters and saturation values calculated for each experiment are in Table 3. At 60ºC, the CO_2 partial pressure of 7.7 bar and H_2S partial pressure of 0.79 mbar were calculated from a total system pressure of 7.9 bar (100 psig). Gas phase additions of H_2S were measured using a colorimetric measurement tube, which has a range of 1 to 240 ppm H_2S with no effect from moisture or temperature. The gas samples were taken just before the gas/liquid mixing point in the system. The iron concentrations were measured by liquid sampling from the pump suction of the system and analyzed with a colorimetric high range iron test analyzer, with a range of 0-10 ppm.

Error analysis of measured data is considered based upon equipment variance and sampling technique. LPR results shown are based upon the final, stable corrosion rate at the end of the test period with error bars in the graphics related to the maximum variation over the last 10 hours of the experiment. WL data presented are averages of multiple coupons with error bars encompassing the maximum and minimum values.

Scanning electron microscopy (SEM) was done with a digital scan generator and an x-ray spectrometer for energy dispersive x-ray spectroscopy (EDS). An electron dispersion spectrograph of a clean AISI 1018 sample showing distinct peaks for iron at 704, 6404, and 7058 eV is shown in Figure 4 for comparison with EDS of coupons with surface films.

RESULTS

100 ppm H_2S

The final corrosion rates measured by LPR and WL in both single phase (SP) and multiphase (MP) for this series of experiments are shown in Figure 5. From the figure, it is observed that the corrosion rate diminishes somewhat from pH 4 to pH 6, and then rises slightly at pH 6.6.

pH 4. A comparison of the corrosion rates measured by all three methods at pH 4 is shown in Figure 6. Comparison of the corrosion rates for weight loss coupons between single phase and multiphase shows a higher corrosion rate for the more turbulent multiphase flow, as expected. Corrosion rate values measured by the three different methods show very good agreement in single phase flow. The respective plot of single-phase LPR with time for this experiment is shown with the WL corrosion rate values in Figure 7. This data shows a rapid decrease in the corrosion rate measured by LPR over the first 24 hours after the probe is exposed to system conditions.

WL coupons retrieved after 96 hrs of exposure to a pH 4 solution with 100 ppm H_2S are shown in Figure 8. These weight loss coupons have a thin black surface film that could be characterized as a protective film because of the low corrosion rates and the fact that initial polish marks can be seen in the contour of the film. The flow direction of all coupons is from the bottom of the page to the top, so the

film of the multiphase coupon was removed due to the turbulence of the flow**,** this is also the only coupon that has localized corrosion. A pit was found with a calculated penetration rate of 3.65 mm/yr; this can be seen visually in the top center of the photograph. This was the only such location found and could not be considered a reproducible event. The corrosion rate calculated from WL coupons was 0.1 mm/yr in single phase and 0.22 mm/yr in multiphase.

The photos in the middle of Figure 8 show the surface features of the film deposited during the experiment while the photos at the bottom of the figure show a cross sectional view to determine the film thickness. The films developed at pH 4 were from 10 to 20 μm thick. The EDS for the film in single phase, Figure 9, shows a peak at 2308 eV, which is an indication of the presence of the element sulfur in the film formed. No change in electronic impedance spectroscopy (EIS) was recorded after 22 hours of exposure to system conditions as seen in Figure 10, which means no change in the surface conditions occurred after the initial film developed.

pH 5. A comparison of the corrosion rates measured by all three methods at pH 5 is shown in Figure 11. The overall corrosion rate has diminished in comparison to pH 4 (Figure 6) with very good agreement between the methods of corrosion rate measurement for both single phase and multiphase. The corrosion rate calculated from WL coupons was 0.04 mm/yr in single-phase flow and 0.08 mm/yr in multiphase flow. The respective plot of LPR with time for single-phase flow in this experiment is shown with the WL corrosion rate values for in Figure 12. This data shows a rapid decrease in the corrosion rate measured by LPR within the first 10 to 15 hours after the probe was exposed to system conditions. This was reflected in the surface films produced on coupons in both single phase and multiphase flow. Figure 13 shows that the coupon surface films at pH 5 provided a uniform surface coverage of 25 to 35 μm in thickness with sulfides detected by EDS as shown in Figure 14. Also under these conditions, EIS measured at different times during the experiment, Figure 15, shows no change in the surface conditions occurred after the initial film developed.

LPR conducted in multiphase flow during pH 4 and pH 5 experiments measured corrosion rates almost 10 times greater than those measured in single phase flow. This was considered to be an artifact of experimentation, as it was determined that the working electrode had become disbonded from the epoxy coating thereby giving the false readings.

pH 6. A comparison of the corrosion rates for all three methods measured at pH 6 is shown in Figure 16. A greater variance is seen between experimental methods and at the same time a smaller variance is seen within each individual method. Even though the weight loss values were less for this experiment, LPR corrosion rate measurements, Figure 17, shows a slightly different trend than previous experiments, in that the corrosion rate measured by the LPR does not drop to a minimum within the first 24 hours. Looking at the surface of the coupons in Figure 18, a uniform dense film with better surface coverage than for pH 4 and 5 has formed. On closer inspection, polish marks are still visible on the surface at 500X magnification and the film thickness is approximately 35 to 40 μm. With the large amount of precipitation that occurred in the bulk, shown by the decrease of dissolved iron concentration in Figure 3 and a diminished sulfide peak for the surface measurement by EDS, Figure 19, a different film was produced in this experiment which was verified by EIS measurements, Figure 20, showing a change in surface characteristics with time.

pH 6.6. A comparison of the corrosion rates measured at pH 6.6 is shown in Figure 21. The corrosion rate for each method is in good agreement and the variance for each method has become minimal. Note also the corrosion rate between single phase and multiphase flows are comparable for this experiment because the sensitivity to the type of flow is reduced as pH increases. LPR data was similar for single-phase flow for this experiment as seen in Figure 22, but due to the variance in the multiphase flow measurement, the LPR data collection continued past the 96 hours. The WL coupons were removed at that time for comparison to the other experiments and it can be seen that the LPR measurements agreed well with the other methods of measurement after the extended time. A surface coverage similar to pH 6 is shown for pH 6.6 in Figure 23, but a different texture is noted in the surface magnification at 500X and the cross sectional thickness of the multiphase film is less than the single phase for this experiment. EDS shows a sulfide peak for the film in Figure 24, confirming iron sulfide was present. EIS measurements, in Figure 25, again verify a different film was produced under higher pH conditions because of the change in surface characteristics with time.

Comparison of Figure 16 to Figure 21 shows a slight change in the corrosion rate for both single phase and multiphase flow conditions by changing the pH of the system from 6 to 6.6. It can be argued that, with the combined supersaturation of both iron sulfide and iron carbonate, a different filming mechanism was observed, which still produced a protective film, but required more time to stabilize. At pH 6.6, precipitation from the bulk was minimal due to lower bulk iron concentration, so film deposition was more dependent upon the corrosion mechanism at the surface of the coupon, which could explain the slight increase in corrosion rate from pH 6 to pH 6.6.

The changes in supersaturation with time for pH 6 and pH 6.6 are shown in Figure 26 and Figure 27, respectively. In both cases, the largest change in the saturation value occurs during the first 30 hours of exposure of the carbon steel corrosion coupons to the system conditions, which agrees with the filming process recorded by LPR and EIS in both cases.

25 ppm H_2S

In a recent report on corrosion in horizontal wet gas flow[8], localized corrosion was observed when partially protective iron carbonate films formed. The set of environmental conditions resulting in this behavior was termed “the grey zone”. In the present study, tests at lower H_2S concentrations for pH 6 were conducted to check if similar behavior could be detected in the presence of H_2S. Figure 28 shows the saturation values for tests at pH 6 with all tests decreasing in iron concentration due to precipitation. The change in supersaturation with time for pH 6 at 25 ppm H_2S is shown in Figure 29. WL coupons retrieved after 240 hrs of exposure to these conditions are shown in Figure 30. The LPR trends for both single phase and multiphase flow conditions, Figure 31, show the decrease in corrosion rate with time over the first 24 to 48 hours of exposure to system conditions. This was similar to previous testing, but the corrosion rate measured by LPR for single phase increased with time after 50 hrs. No apparent reason for this increase in corrosion rate was observed on the probe surface after removal from the system, but the EDS for the WL under the same conditions, Figure 32, did not detect a significant amount of sulfides in the film formed, which could be indicative of the domination of an iron carbonate film under these conditions. Yet, EIS conducted during the experiment for single phase, Figure 33, shows the formation of a surface film that was very protective, after 65 hours, which is similar to the behavior of a thin dense mackinawite film. The corrosion rate for multiphase flow

conditions remained stable after 96 hours of experimentation, indicative of an adherent film, confirmed in the Nyquist plot of Figure 34.

WL corrosion rates for these coupons were approximately 0.1 mm/yr. A comparison of corrosion rates obtained at pH 6 shows no effect of the concentration of H_2S in the range 25 to 100 ppm on final corrosion rates under these conditions. Even though both experiments ended with similar iron carbonate saturation values in the "grey zone," no localized corrosion was observed even with the extended test time of 240 hours.

CONCLUSIONS

1. For concentrations of H_2S < 500 ppm in the gas phase and for pH<5, when there is no precipitation of carbonate or sulfide films, the data strongly suggest that the presence of even very small amounts of H_2S (10 ppm in the gas phase) will lead to rapid and significant reduction in the CO_2 corrosion rate. At higher H_2S concentrations this trend is arrested and somewhat reversed.

2. A change in the pH of the system from 4 to 6 has little effect on the corrosion rate as measured by LPR and WL in either single phase or multiphase flow conditions.

3. At 60ºC, 7.9 bar, 25ppm H_2S, and pH 6, protective adherent films were formed in single phase and multiphase flow conditions and no localized corrosion was observed.

4. No effect of H_2S concentration (in the range 25 to 100 ppm) on the protectiveness of the surface films was observed.

ACKNOWLEDGEMENTS

The authors would like to acknowledge the contribution of a consortium of companies whose continuous financial support and technical guidance made this research possible. They are: BP, ConocoPhillips, ENI, Petrobras, Saudi Aramco, Shell, Total, Champion Technologies, Clariant, MI Technologies and Nalco. We would also like to thank our colleagues: Wei Sun and Kun-Lin Lee, PhD candidates at the Institute for Corrosion and Multiphase Technology, for their help with equilibrium constants and speciation calculations.

REFERENCES

1. Ikeda, A., Ueda, M., and Mukai, S., "Influence of Environmental Factors on Corrosion in CO_2 Source Well," Advances in CO_2 Corrosion, Vol. 2, 1985.

2. Valdes, A., Case, R, Ramirez, M., and Ruiz, A., "The Effect of Small Amounts of H_2S on CO_2 Corrosion of a Carbon Steel," CORROSION/98, paper 22, NACE International, Houston, TX, 1998.

3. Kvarekval, J., "The Influence of Small Amounts of H_2S on CO_2 Corrosion of Iron and Carbon Steel," EUROCORR '97, Trondheim, Norway.

4. Brown, B., Lee, K.-L., Nesic, S., "Corrosion in Multiphase Flow Containing Small Amounts of H_2S", CORROSION/03, paper 03341, NACE International, Houston, TX, 2003.

5. Benning, L.G., Wilkin, R.T., Barnes, H.L., "Reaction pathways in the Fe-S system below 100ºC," Chemical Geology, v. 167, 2000, pp25-51

6. IUPAC: Chemical Data Series No. 21, Stability constants of Metal-Ion Complexes. Par A: Inorganic ligands. Pergamon Press.

7. Brown, B., Schubert, A., "The Design and Development of a Large-Scale Multiphase Flow Loop for the Study of Corrosion in Sour Gas Environments," CORROSION/02, paper 02502, NACE International, Houston, TX, 2002.

8. Sun, Y., "Localized Corrosion in Horizontal Wet Gas Flow," Ohio University, PhD dissertation, June 2003.

TABLES

Table 1. TEST MATRIX

Parameter	**Conditions**
CO_2 partial pressure	0.77 MPa (7.7 bar)
Solution	1% NaCl, pH 4, 5, 6, & 6.6
Corrosion Rate Measurement	AISI 1018 weight loss Electrical Resistance Linear Polarization Resistance
single-phase flow	V_{sl} = 1.0 m/s
two-phase flow	V_{sg} = 3 m/s V_{sl} = 1.0 m/s
Temperature	60ºC
Test Time	96 hrs (4 days)
H_2S gas phase concentration	25 and 100 ppm

Table 2. MATERIAL CHEMICAL COMPOSITION

Material	C	Si	Mn	P	S	Ni	Cr	Mo
AISI 1018	0.20%	0.044%	0.90%	0.017%	0.012%	0.044%	0.061%	0.018%

Table 3. SATURATION VALUES

Mackinawite ($SS(FeS_{1-x})$) and iron carbonate ($SS(FeCO_3)$) saturation values calculated from experimental conditions at the beginning and end of each test. (0.79 MPa CO_2, 60ºC, V_{sg} = 3.0m/s, V_{sl} = 1.0m/s, 1% NaCl)

pH	H_2S ppm:	Fe^{2+} ppm:	$SS(FeS_{1-x})$ begin	$SS(FeS_{1-x})$ end	$SS(FeCO_3)$ begin	$SS(FeCO_3)$ end
4	100	56 - 68	< 0.1	0.3	< 0.1	< 0.1
5	100	68 - 62	6.6	2.0	0.4	0.2
6	25	16 - 11	6.5	5.0	2.2	1.8
6	100	55 - 10	501.4	11.3	36.8	1.0
6.6	100	8 - 2	496.8	132.8	37.2	11.8

FIGURES

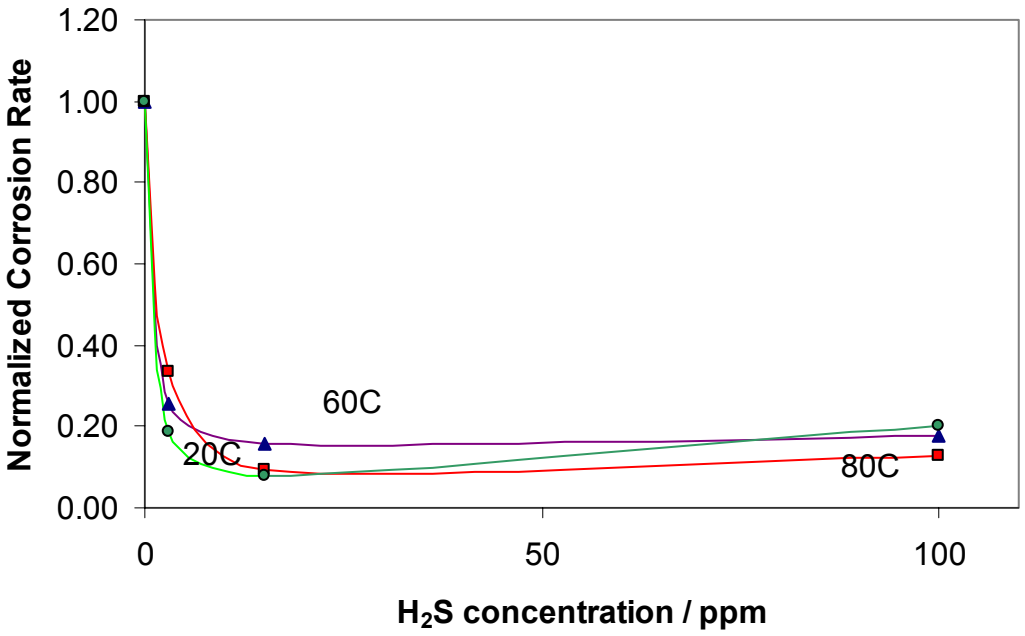

Figure 1. Effect of low concentrations of H_2S on the CO_2 corrosion rate in the absence of iron sulphide precipitation. (20°C, RCE, 1 bar CO_2; 60°C and 80°C, flowloop, 7 bar CO_2; ppm refers to H_2S concentration in the gas phase).

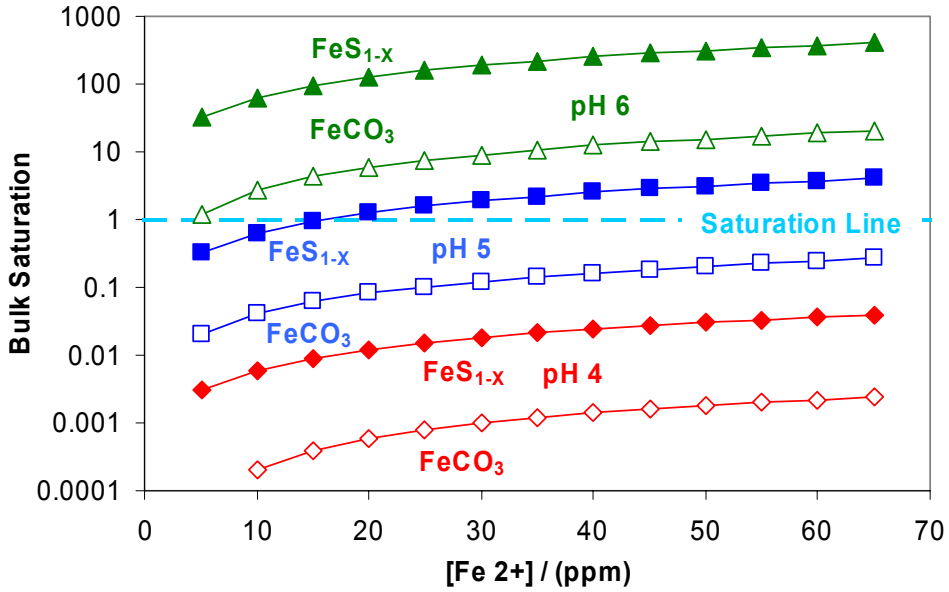

Figure 2. Theoretical calculation of bulk solution saturation values at test conditions. (0.79 MPa CO_2, 60ºC, 100 ppm H_2S, 1% NaCl)

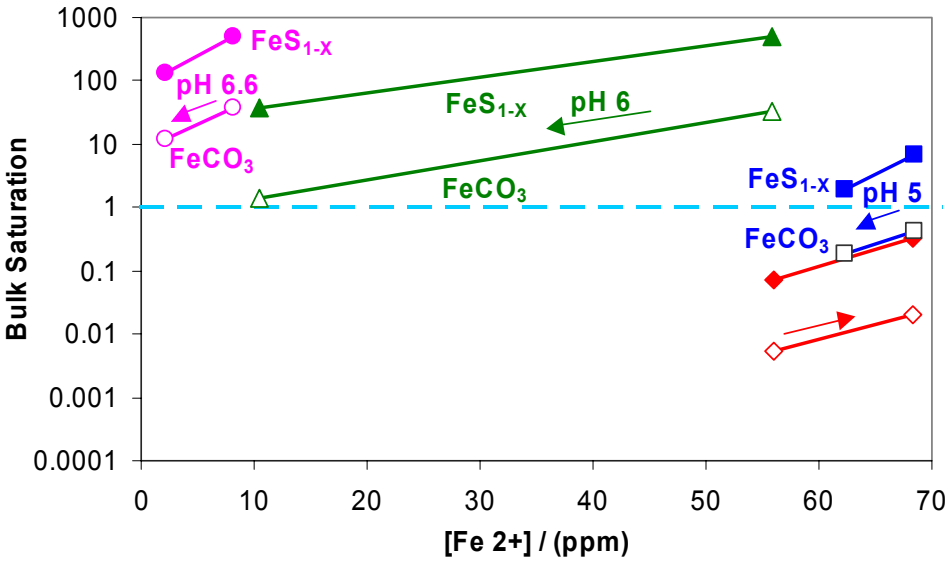

Figure 3. Bulk solution saturation values calculated from system parameter measurements at the beginning and end of each experiment. The arrows' direction is from the beginning to the end of each experiment. (0.79 MPa CO_2, 60ºC, 100 ppm H_2S, 1% NaCl)

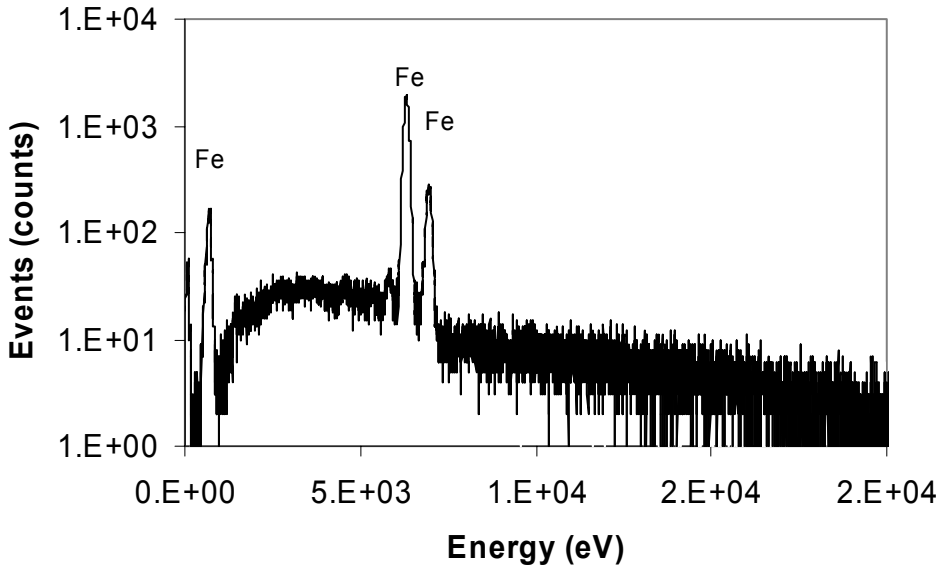

Figure 4. Electron dispersion spectroscopy (EDS) of a clean metal surface, AISI 1018.

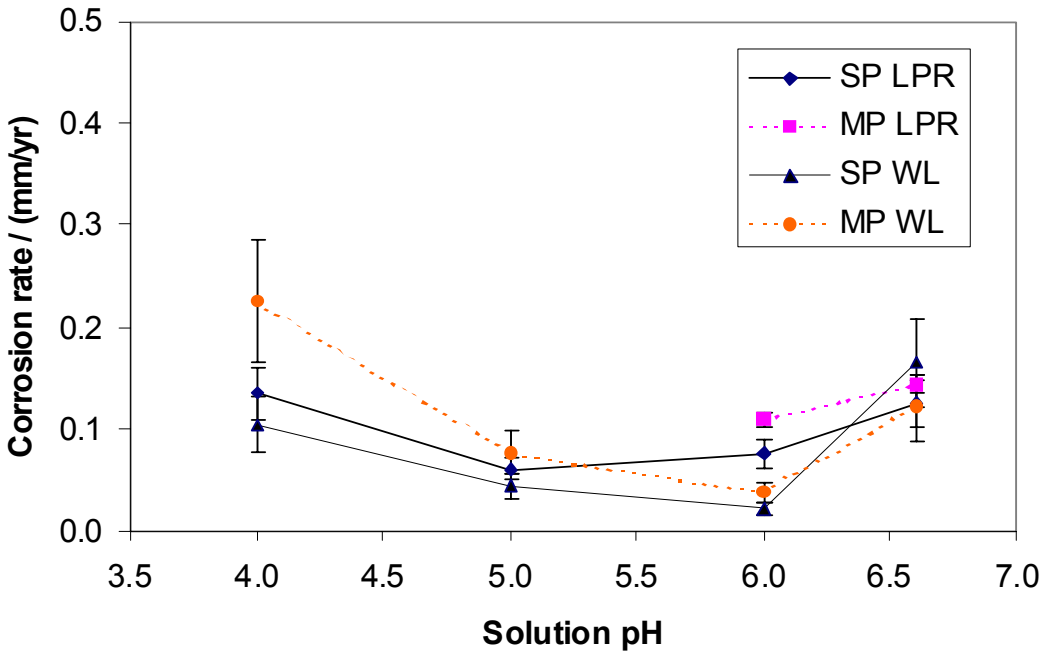

Figure 5. Final corrosion rate after 96 hours of exposure to system conditions for LPR and WL values. (0.79 MPa CO_2, 60ºC, V_{sg} = 3.0m/s, V_{sl} = 1.0m/s, 100 ppm gas phase concentrate ion of H_2S, 1% NaCl)

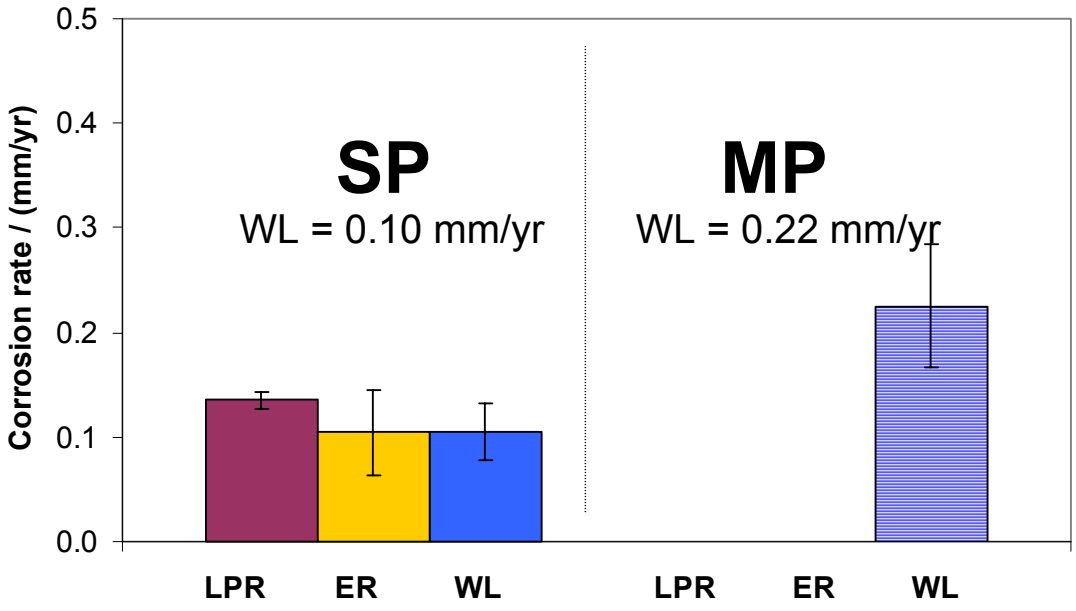

Figure 6. Corrosion rates after 96 hours of exposure to system conditions, pH 4. (0.79 MPa CO_2, 60ºC, V_{sg} = 3.0m/s, V_{sl} = 1.0m/s, 100 ppm H_2S, SP: single phase, MP: multiphase) NA: not available.

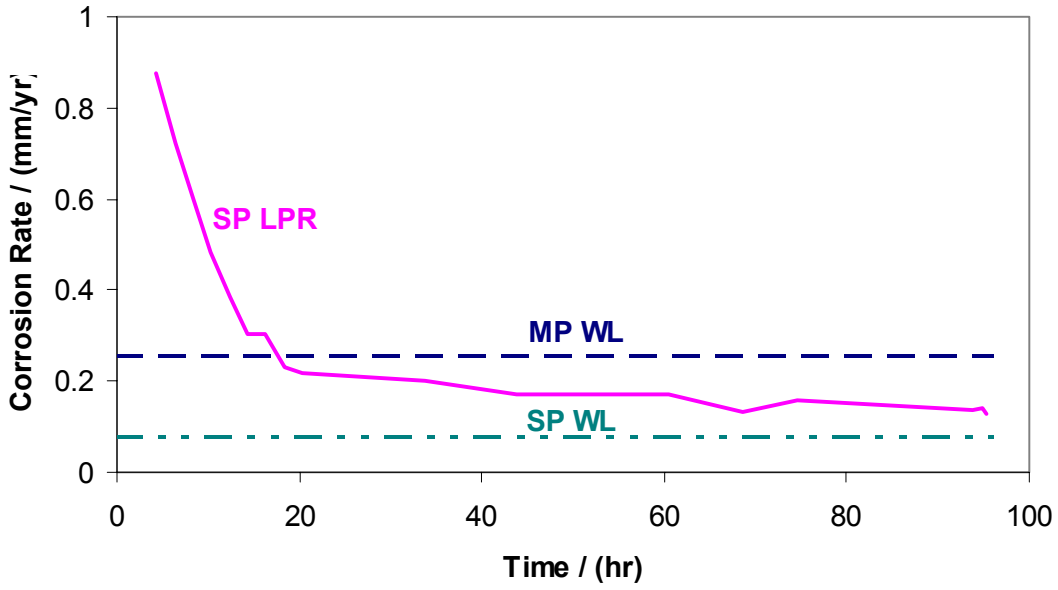

Figure 7. Corrosion rates measured by LPR and WL exposed to 100 ppm H_2S in pH 4 solution. (0.79 MPa CO_2, 60°C, 1% NaCl, V_{sl} = 1.0m/s)

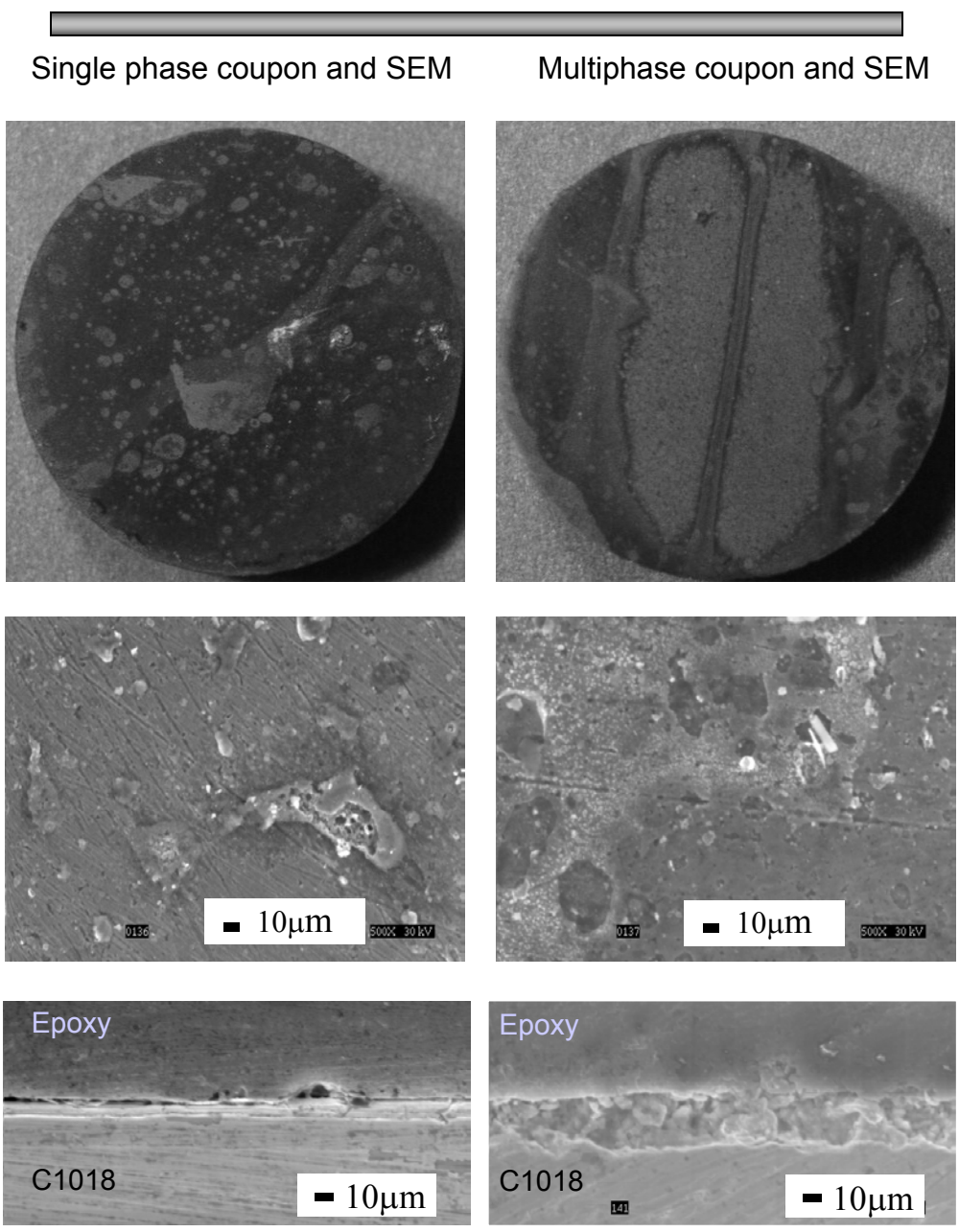

Figure 8. Weight loss coupons exposed to 100 ppm H_2S in pH 4 solution. Single phase on the left, multiphase on the right. (0.79 MPa CO_2, 60°C, 1% NaCl, V_{sg} = 3.0m/s, and/or V_{sl} = 1.0m/s)

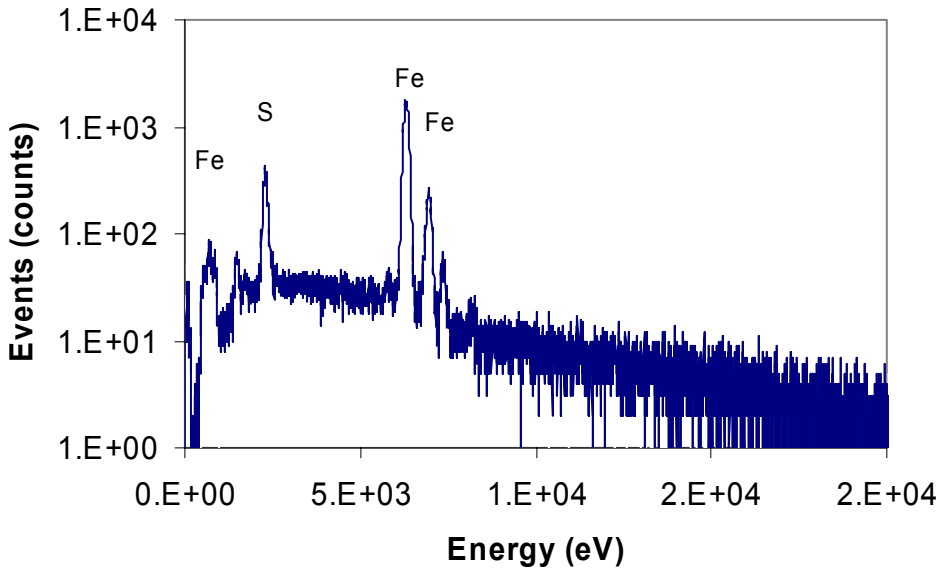

Figure 9. EDS of coupon surface after exposure to 100 ppm H_2S in pH 4 solution Single phase. (0.79 MPa CO_2, 60°C, 1% NaCl, and V_{sl} = 1.0m/s)

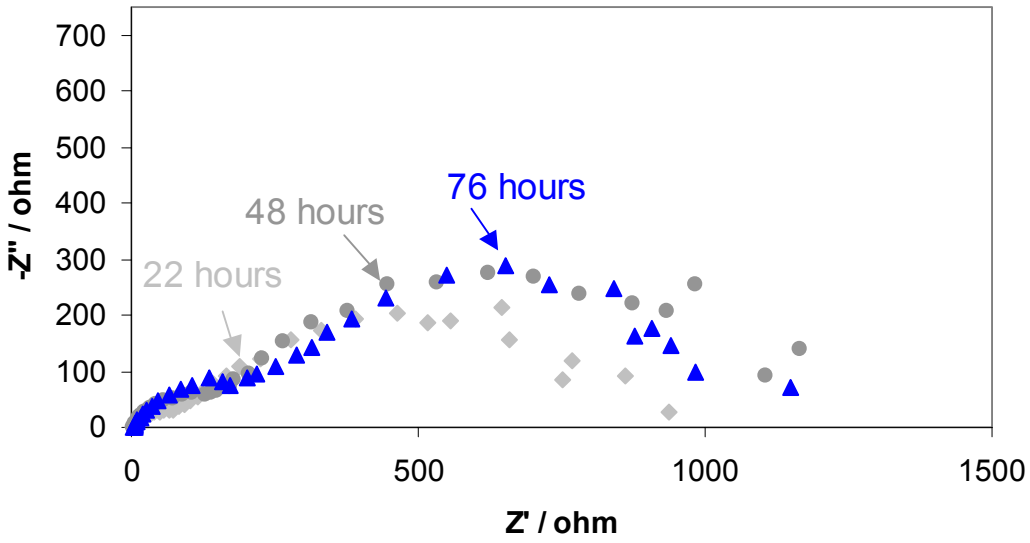

Figure 10. Nyquist plot for single phase flow with time in 100 ppm H_2S in pH 4 Single phase solution. (0.79 MPa CO_2, 60°C, 1% NaCl, and V_{sl} = 1.0m/s)

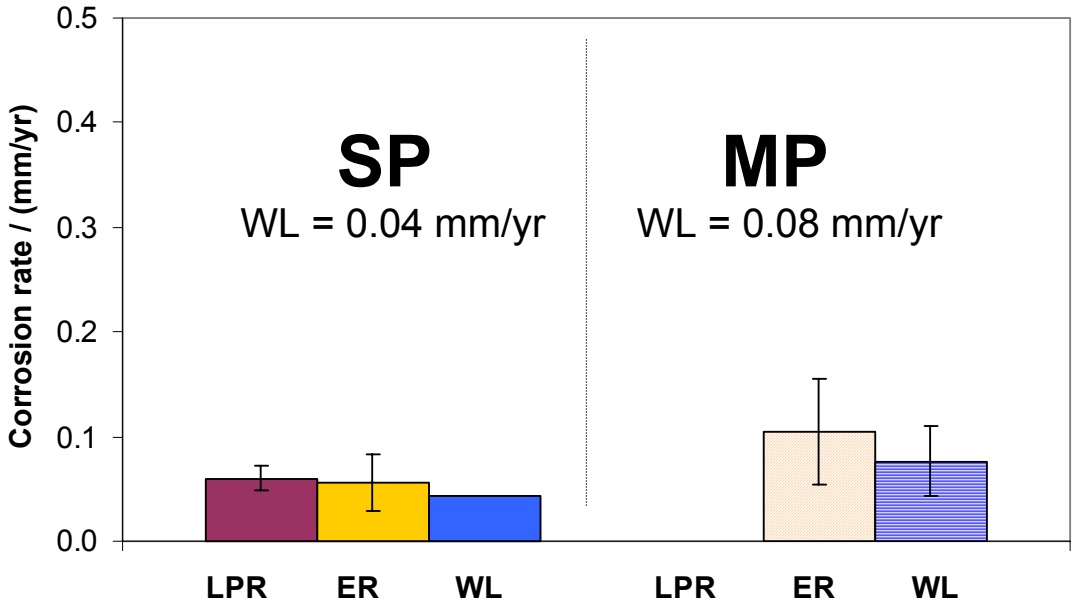

Figure 11. Corrosion rate after 96 hours of exposure to system conditions, pH 5. (0.79 MPa CO_2, 60ºC, V_{sg} = 3.0m/s, V_{sl} = 1.0m/s, 100 ppm H_2S, SP: single phase, MP: multiphase) NA: not available.

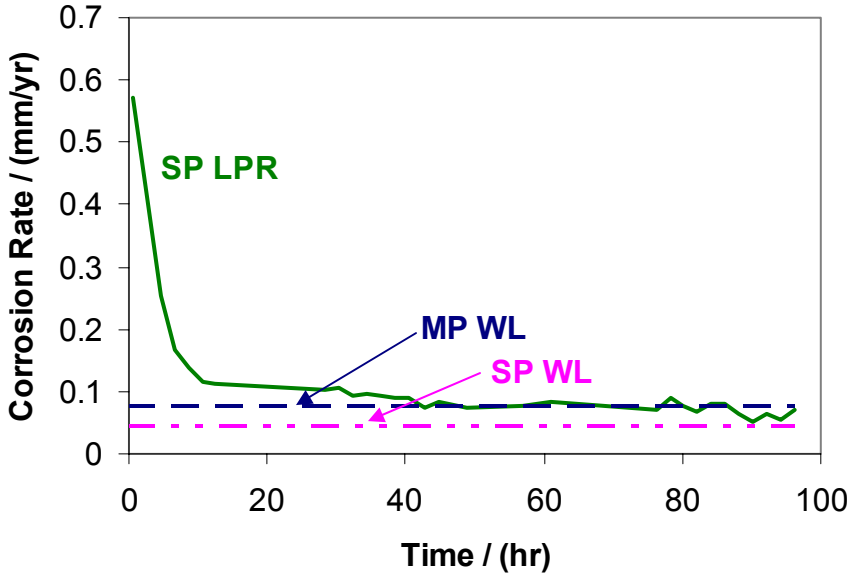

Figure 12. Corrosion rates measured by LPR and WL exposed to 100 ppm H_2S in pH 5 solution. (0.79 MPa CO_2, 60°C, 1% NaCl, V_{sl} = 1.0m/s)

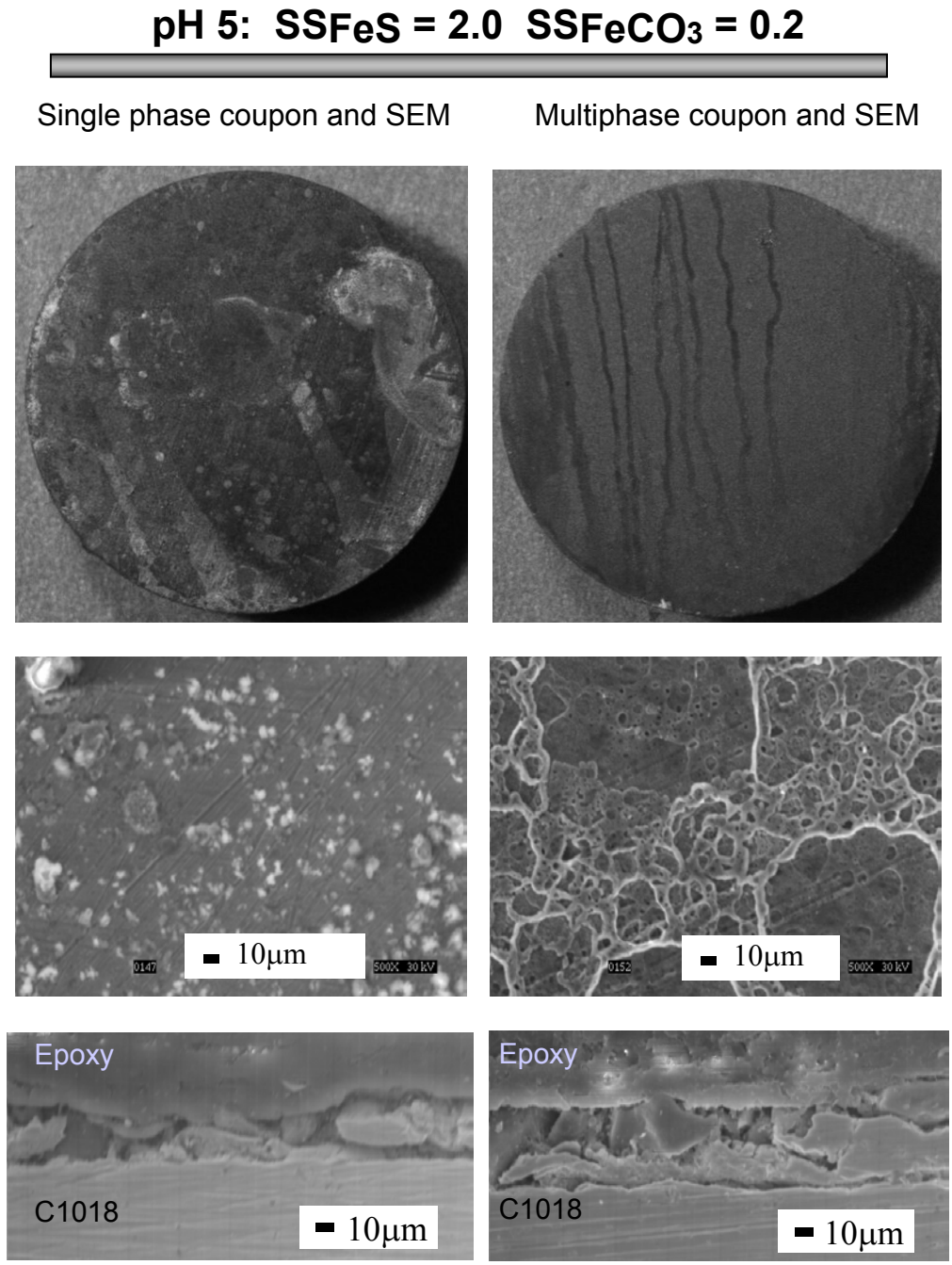

Figure 13. Weight loss coupons exposed to 100 ppm H_2S in pH 5 solution. Single phase on the left, multiphase on the right, 500X magnification. (0.79 MPa CO_2, 60°C, 1% NaCl, V_{sg} = 3.0m/s, and/or V_{sl} = 1.0m/s, 96 hrs.)

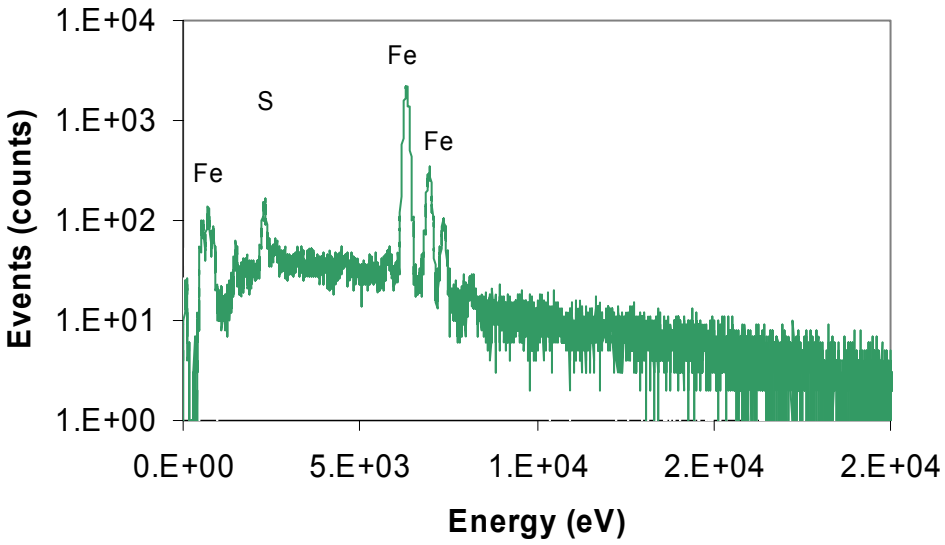

Figure 14. EDS of coupon surface after exposure to 100 ppm H_2S in pH 5 solution Single phase. (0.79 MPa CO_2, 60°C, 1% NaCl, V_{sl} = 1.0m/s, 96 hrs.)

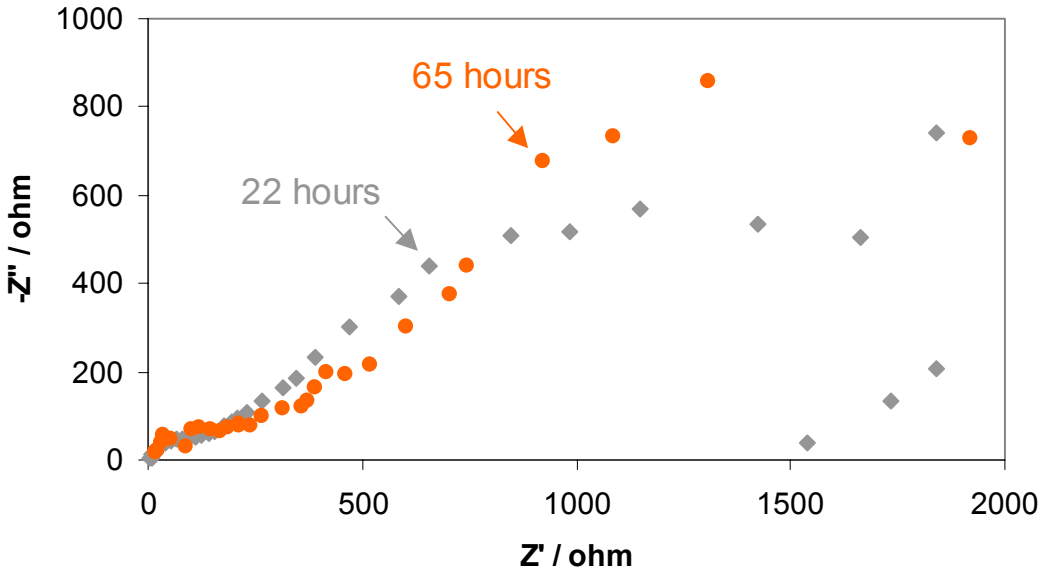

Figure 15. Nyquist plot for single phase flow with time in 100 ppm H_2S in pH 5 single phase solution. (0.79 MPa CO_2, 60°C, 1% NaCl, and V_{sl} = 1.0m/s)

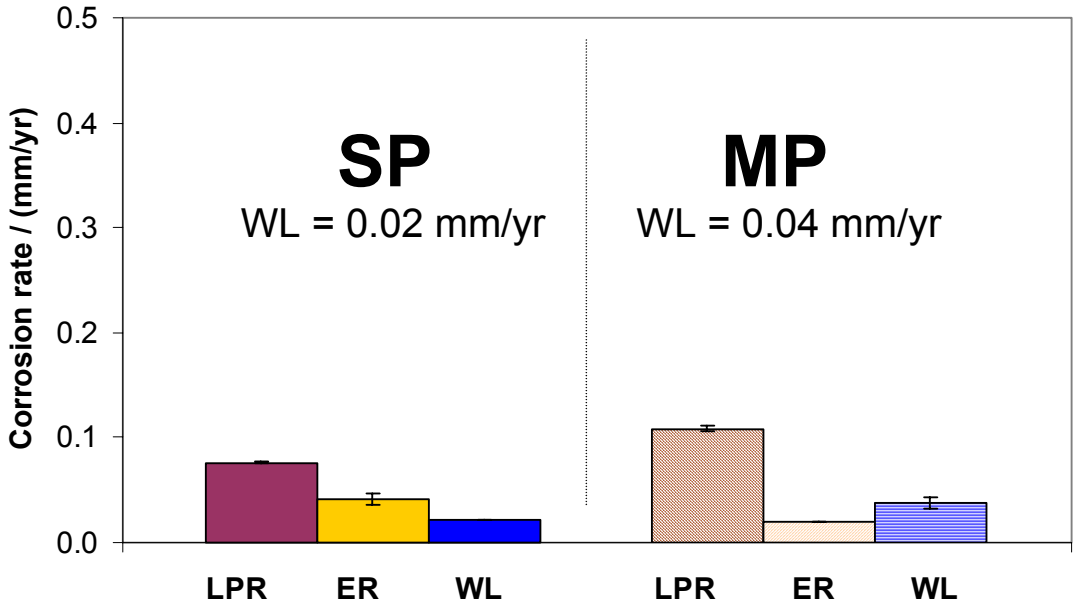

Figure 16. Corrosion rate after 96 hours of exposure to system conditions, pH 6. (0.79 MPa CO_2, 60ºC, V_{sg} = 3.0m/s, V_{sl} = 1.0m/s, 100 ppm H_2S, SP: single phase, MP: multiphase)

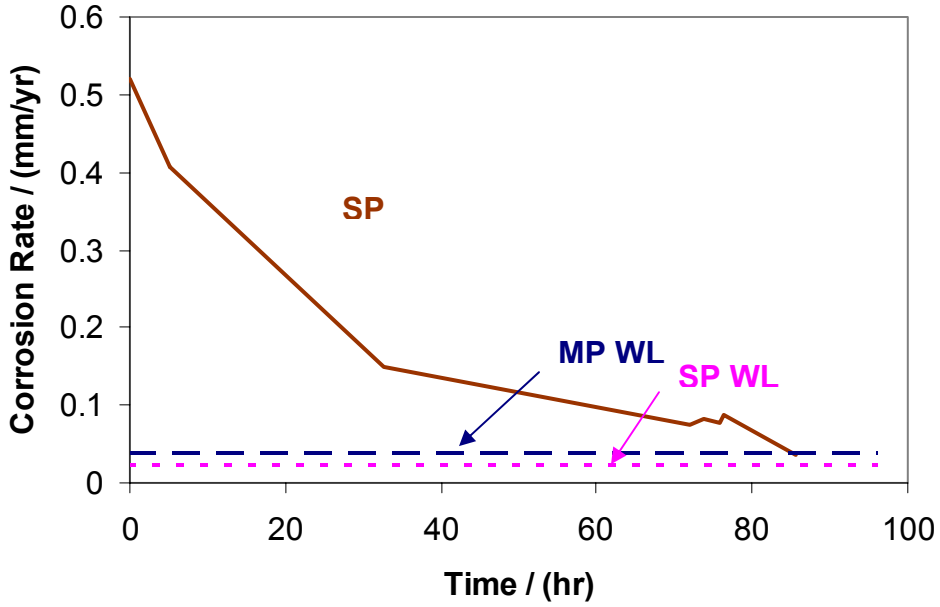

Figure 17. Corrosion rates measured by LPR and WL exposed to 100 ppm H_2S in pH 6 solution. (0.79 MPa CO_2, 60°C, 1% NaCl, V_{sg} = 3.0m/s, V_{sl} = 1.0m/s) .

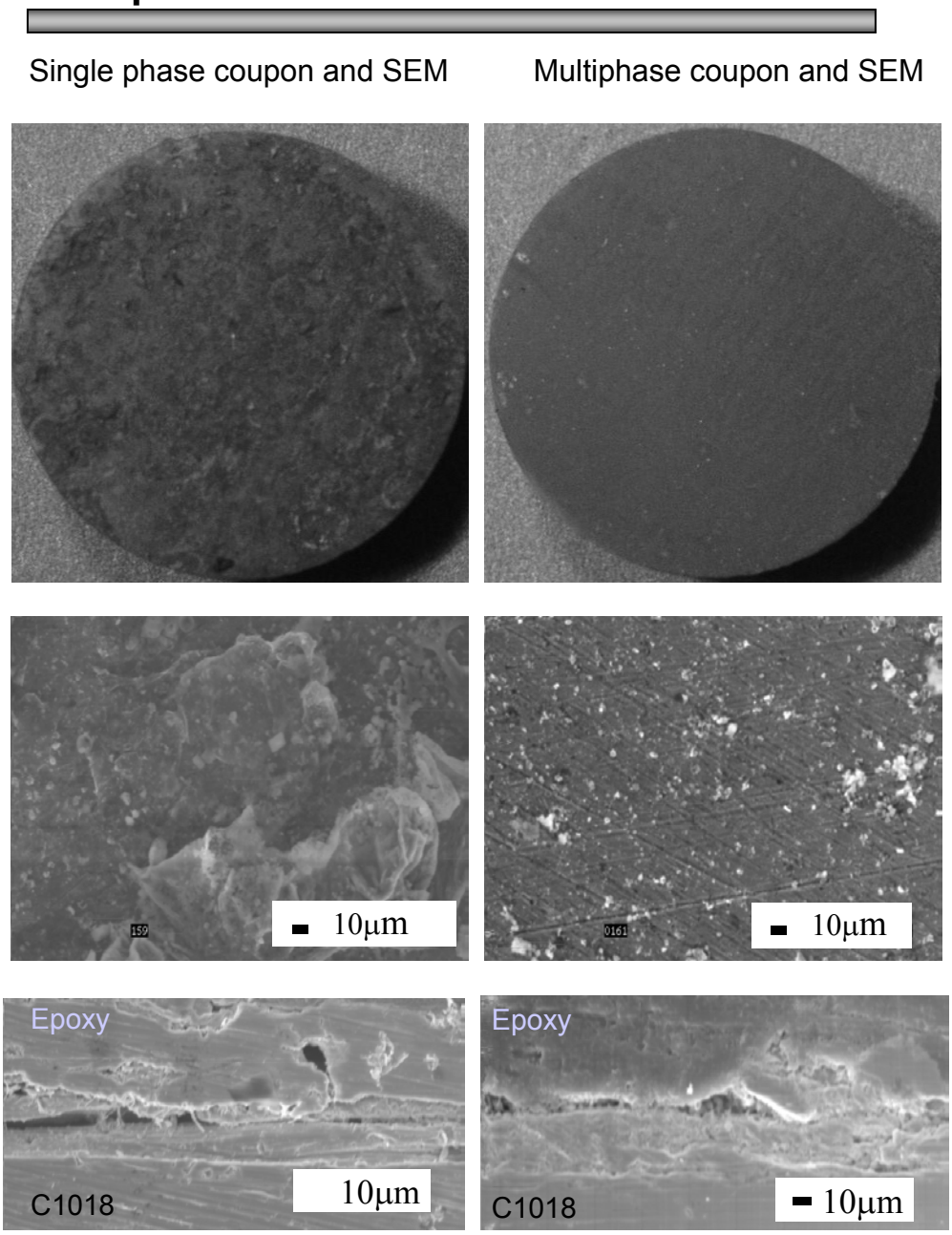

Figure 18. Weight loss coupons exposed to 100 ppm H_2S in pH 6 solution. Single phase on the left, multiphase on the right, 500X magnification. (0.79 MPa CO_2, 60°C, 1% NaCl, V_{sg} = 3.0m/s, and/or V_{sl} = 1.0m/s)

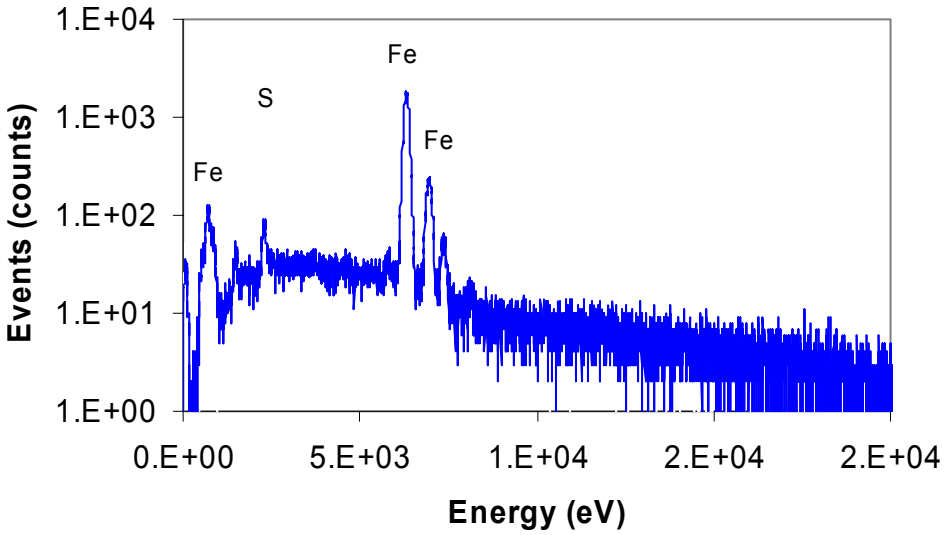

Figure 19. EDS of coupon surface after exposure to 100 ppm H_2S in pH 5 solution Single phase. (0.79 MPa CO_2, 60°C, 1% NaCl, V_{sl} = 1.0m/s, 96 hrs.)

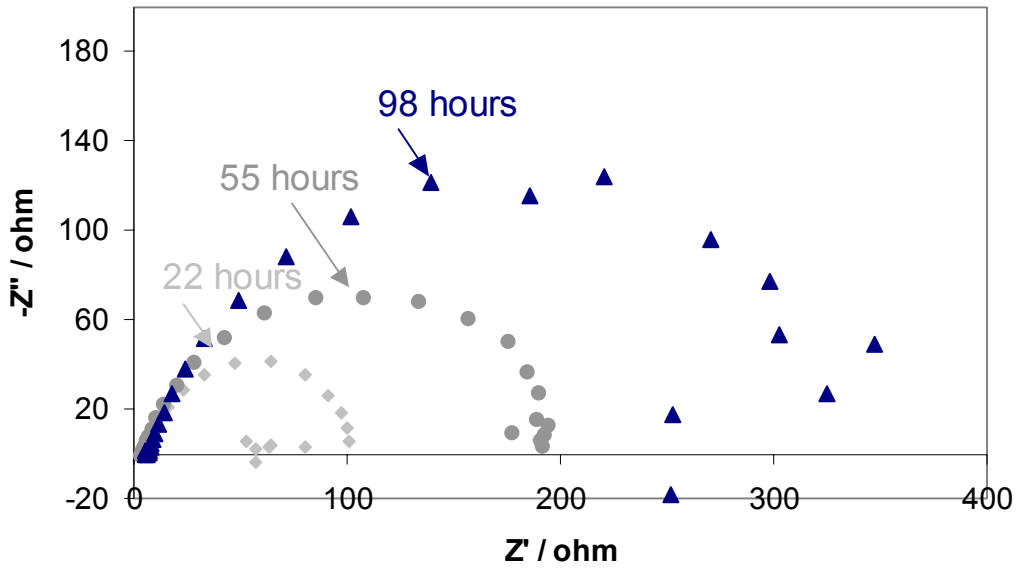

Figure 20. Nyquist plot for single phase flow with time in 100 ppm H_2S in pH 6 single phase solution. (0.79 MPa CO_2, 60°C, 1% NaCl, and V_{sl} = 1.0m/s)

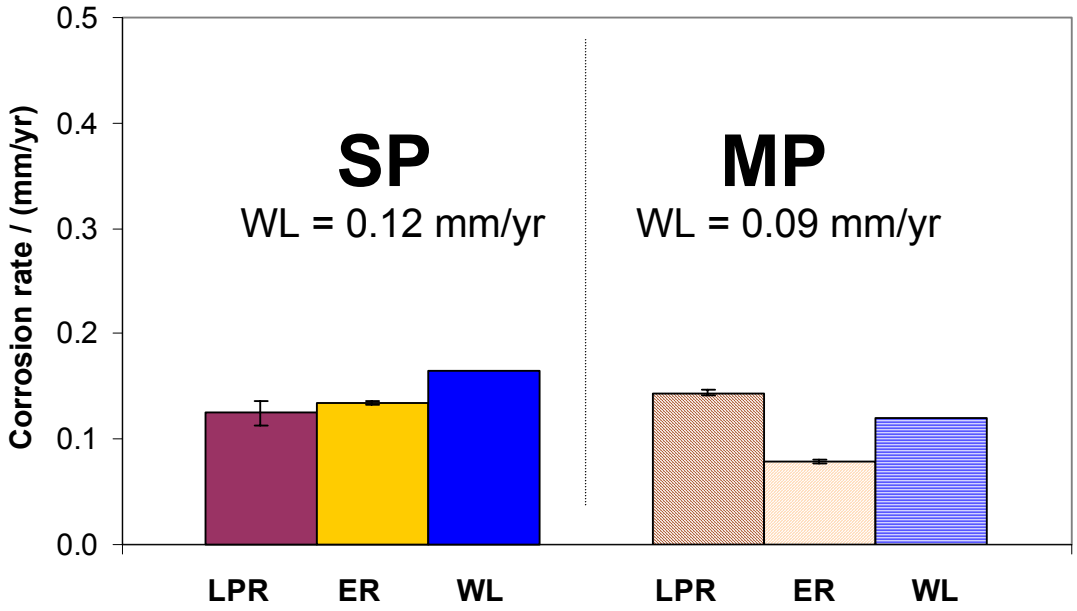

Figure 21. Corrosion rate after 96 hours of exposure to system conditions, pH 6.6. (0.79 MPa CO_2, 60ºC, V_{sg} = 3.0m/s, V_{sl} = 1.0m/s, 100 ppm H_2S, SP: single phase, MP: multiphase)

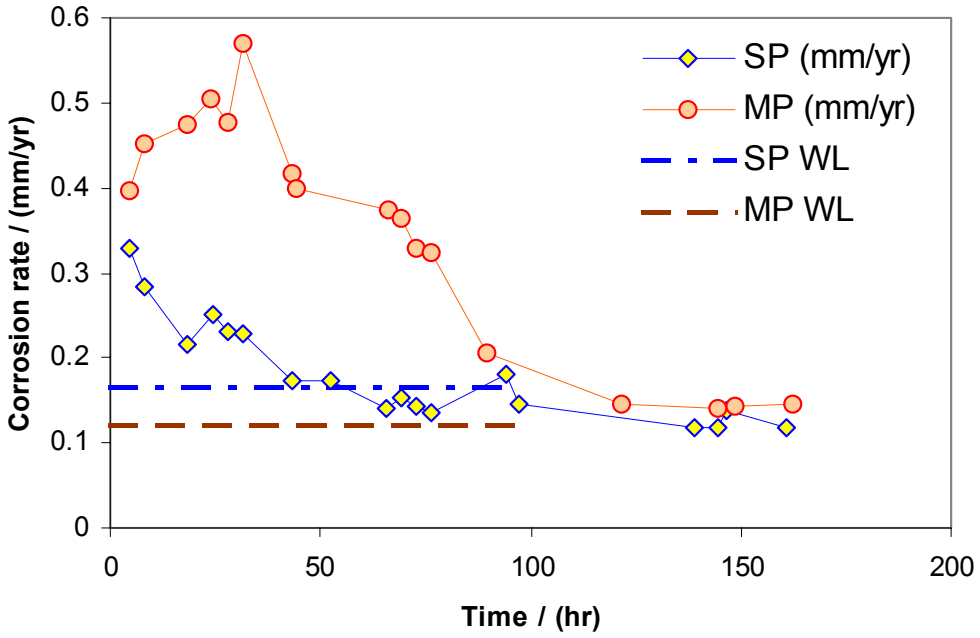

Figure 22. Corrosion rates measured by LPR and WL exposed to 100 ppm H_2S in pH 6.6 solution. (0.79 MPa CO_2, 60°C, 1% NaCl, V_{sl} = 1.0m/s)

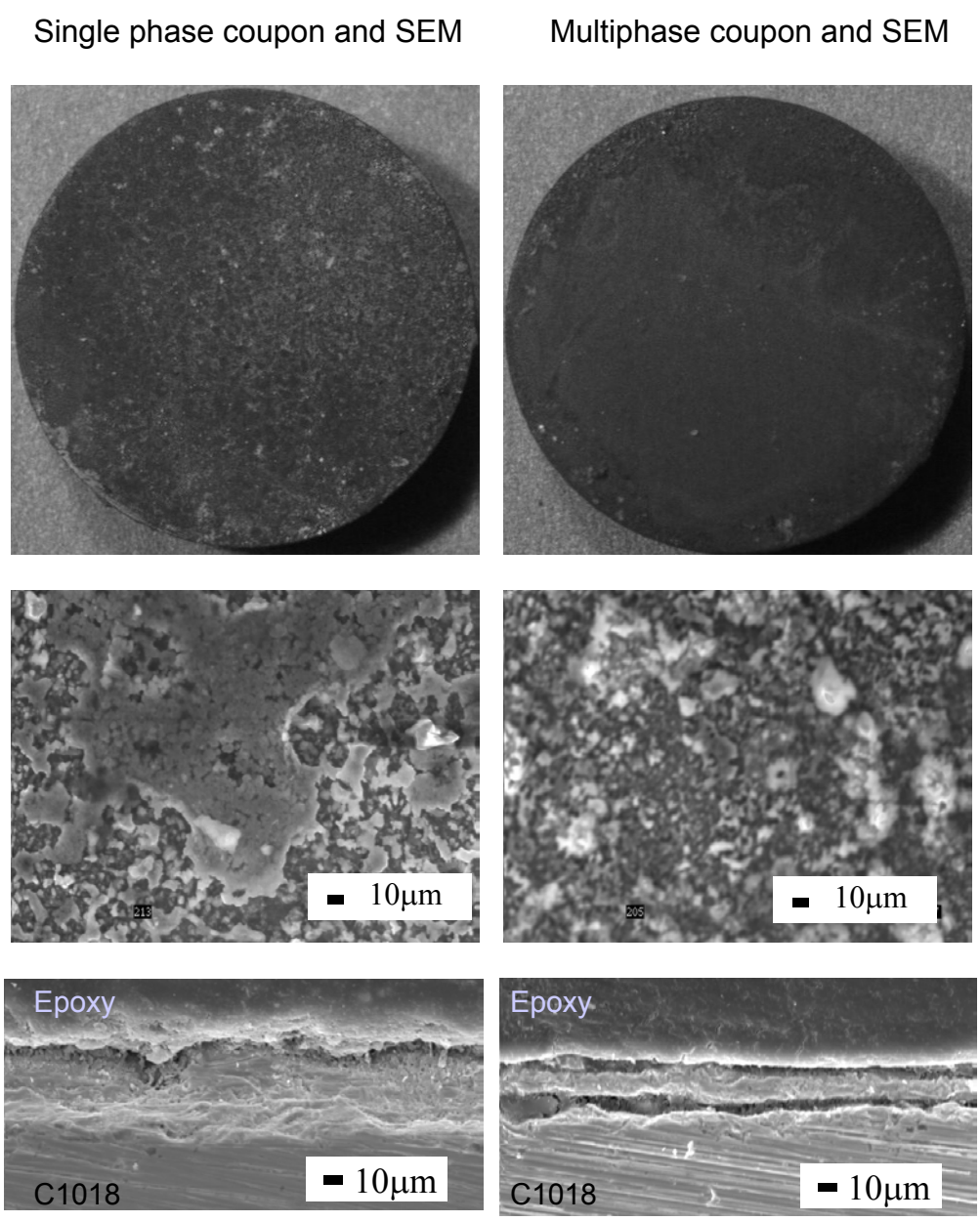

Figure 23. Weight loss coupons exposed to 100 ppm H_2S in pH 6.6 solution. Single phase on the left, multiphase on the right, 500X magnification. (0.79 MPa CO_2, 60°C, 1% NaCl, V_{sg} = 3.0m/s, and/or V_{sl} = 1.0m/s)

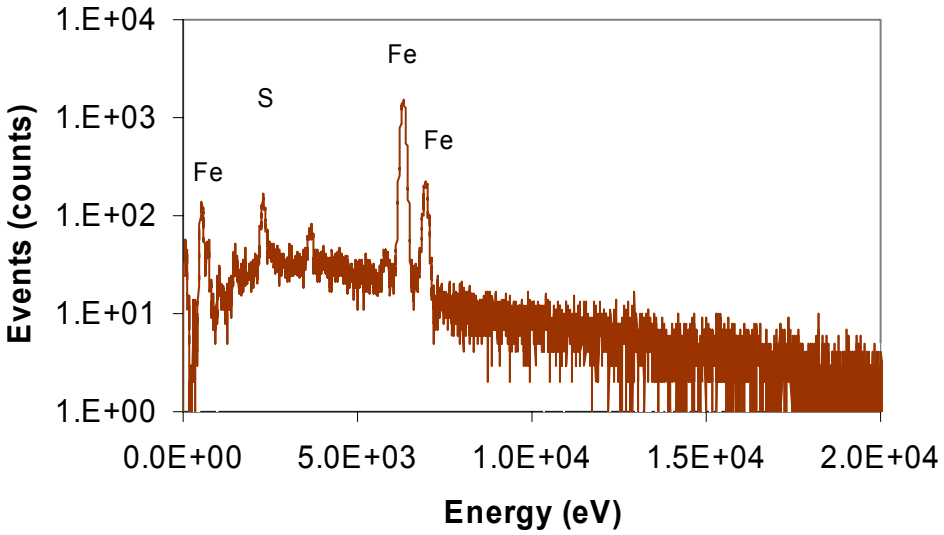

Figure 24. EDS of coupon surface after exposure to 100 ppm H_2S in pH 6.6 solution Single phase. (0.79 MPa CO_2, 60°C, 1% NaCl, V_{sl} = 1.0m/s, 96 hrs.)

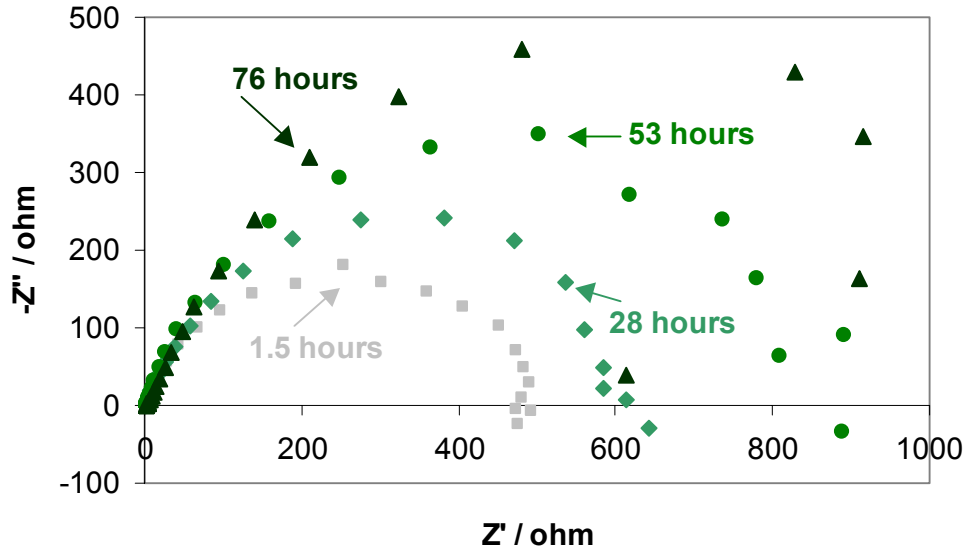

Figure 25. Nyquist plot for single phase flow with time in 100 ppm H_2S in pH 6.6 single phase solution. (0.79 MPa CO_2, 60°C, 1% NaCl, and V_{sl} = 1.0m/s)

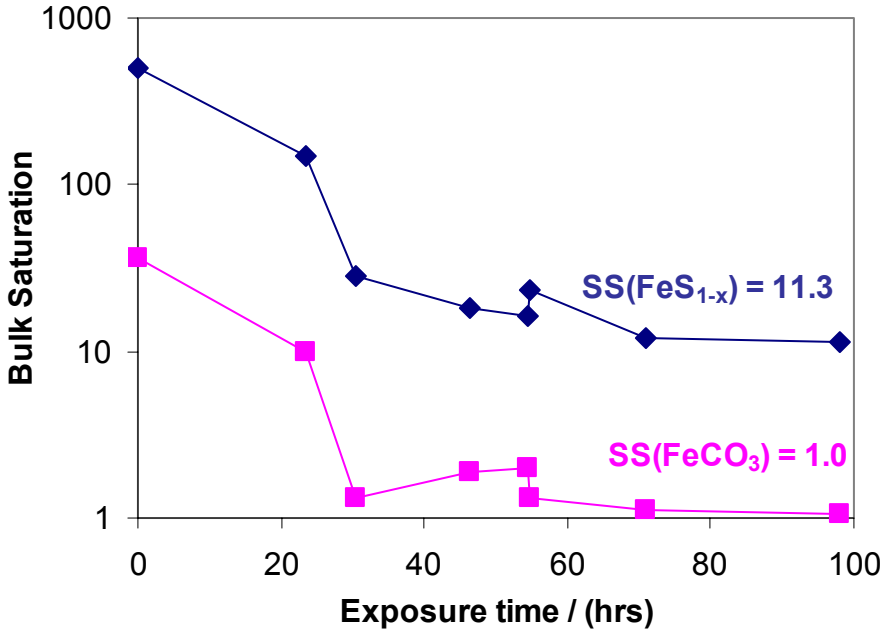

Figure 26. Variation of bulk saturation with time, pH 6.0, 100 ppm H_2S,

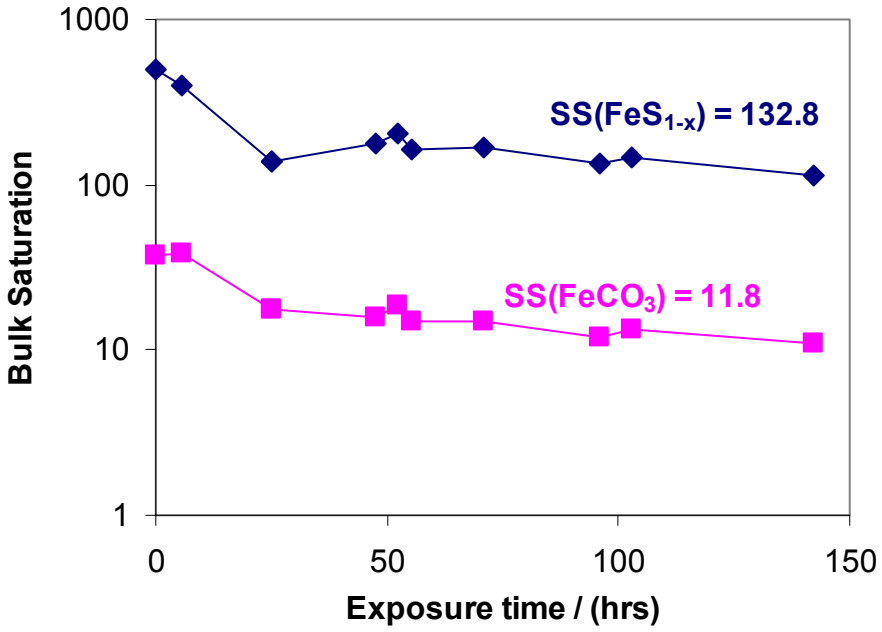

Figure 27. Variation of bulk saturation with time, pH 6.6, 100 ppm H_2S.

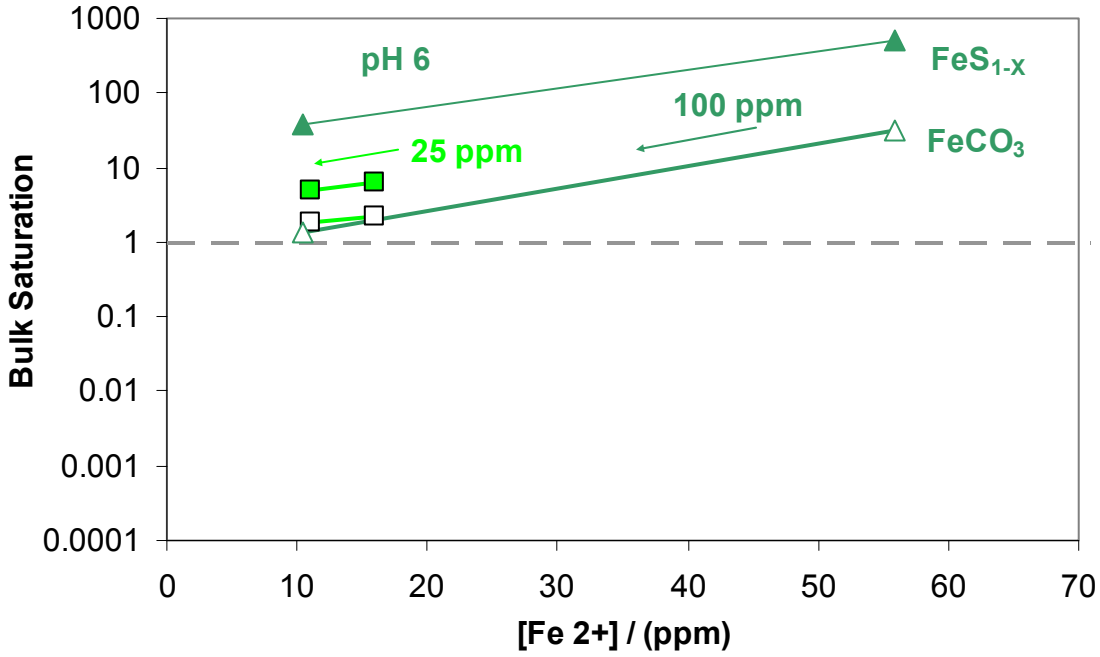

Figure 28. Tests in the "Grey Zone" for $FeCO_3$, bulk saturation for the beginning and end of experiments: pH 6; 5, 25, and 100 ppm H_2S. (0.79 MPa CO_2, 60°C, 1% NaCl, V_{sg} = 3.0m/s, and/or V_{sl} = 1.0m/s)

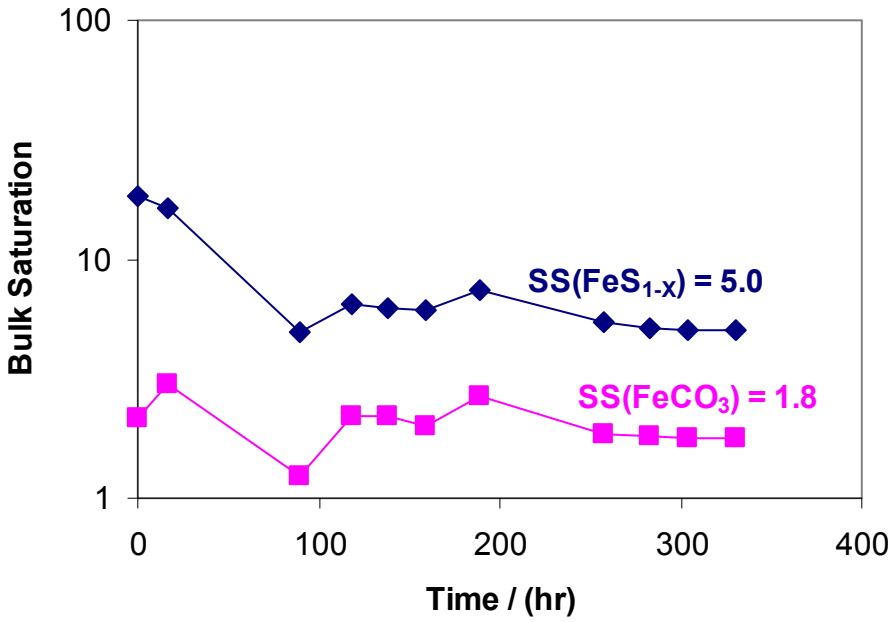

Figure 29. Variation of bulk saturation with time, pH 6, 25 ppm H_2S

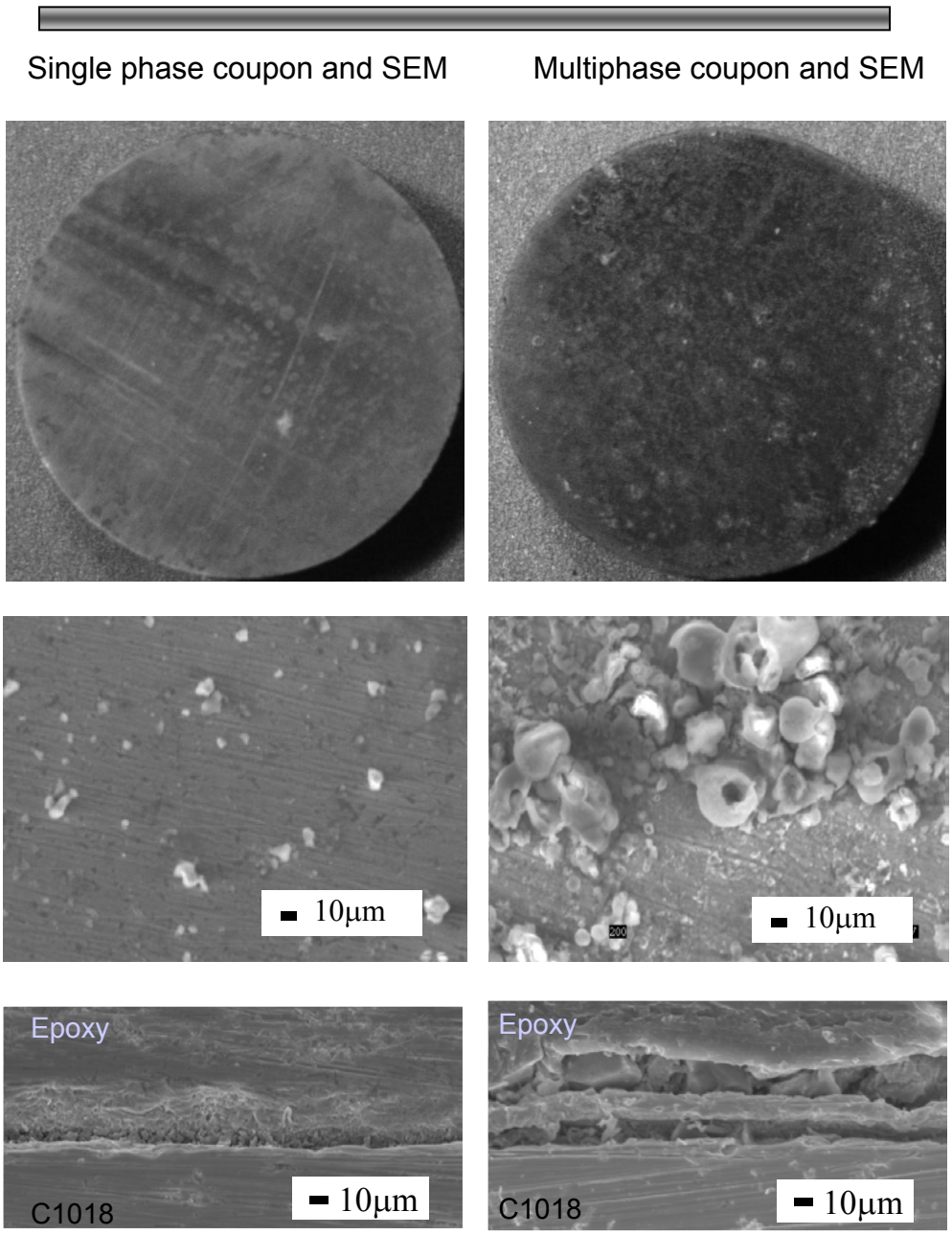

Figure 30. Weight loss coupons exposed to 25 ppm H_2S in pH 6 solution. Single phase on the left, multiphase on the right, 500X magnification. (0.79 MPa CO_2, 60°C, 1% NaCl, V_{sg} = 3.0m/s, and/or V_{sl} = 1.0m/s)

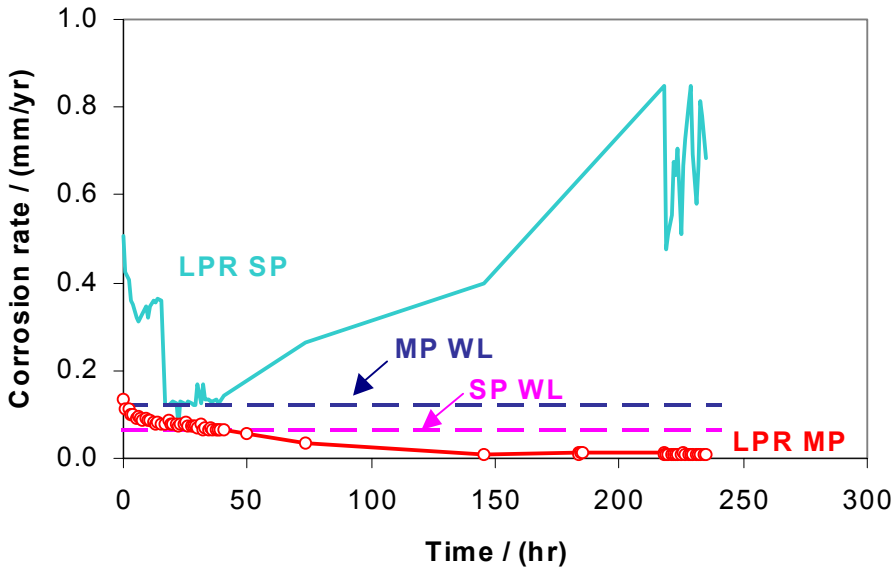

Figure 31. Corrosion rates measured by LPR and WL exposed to 25 ppm H_2S in pH 6.0 solution. (0.77 MPa CO_2, 60°C, 1% NaCl, V_{sl} = 1.0m/s)

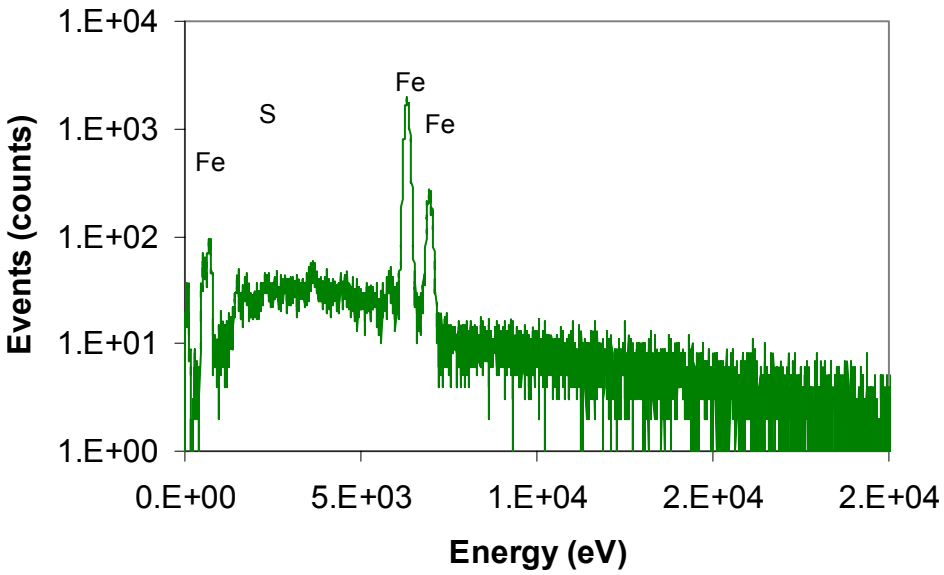

Figure 32. EDS, pH 6, 25 ppm H_2S, single phase flow exposure

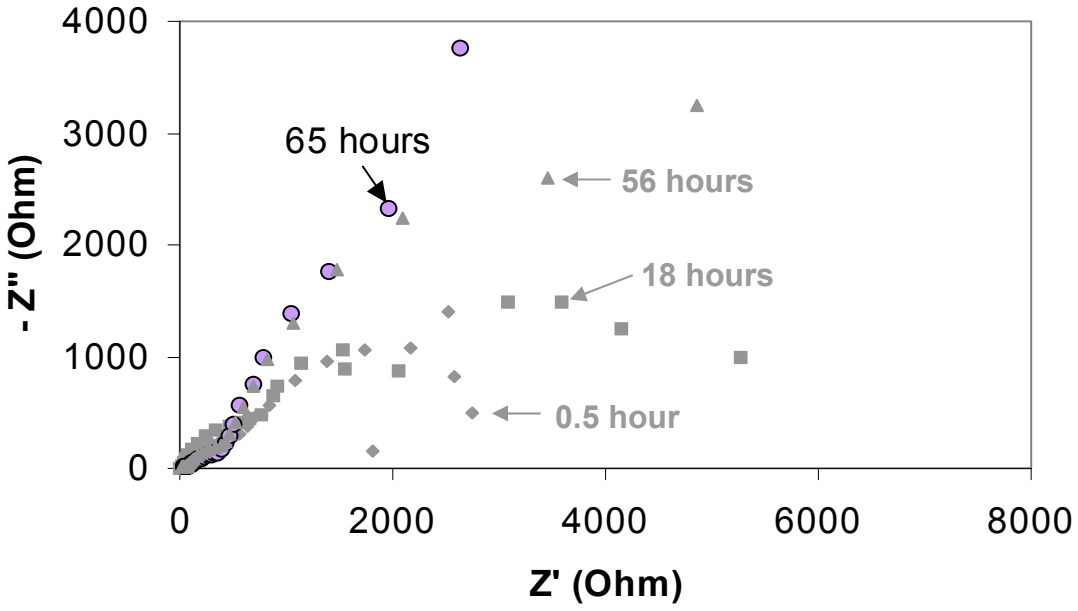

Figure 33. Nyquist plot for single phase flow with time in 25 ppm H_2S in pH 6 single phase. (0.79 MPa CO_2, 60°C, 1% NaCl, and V_{sl} = 1.0m/s)

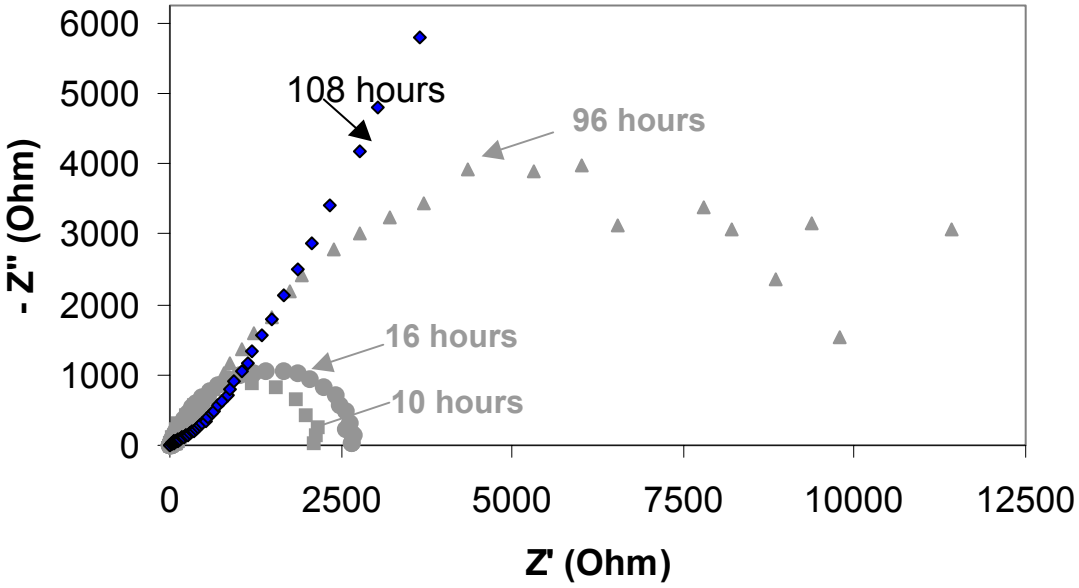

Figure 34. Nyquist plot for for multiphase flow with time in 25 ppm H_2S in pH 6. (0.79 MPa CO_2, 60°C, 1% NaCl, and V_{sl} = 1.0m/s)